Spinodal decomposition in the Fe-Cr alloys: Effect of inhomogeneous elasticity and dislocation

Wooseob Shin [a], Jeonghwan Lee[a], Kunok Chang [a*]
[a]*Department of Nuclear Engineering, KyungHee University, Yong-in city, Korea*
[*]*Corresponding author: kunok.chang@khu.ac.kr*

1. Introduction

α' precipitate hardening in Fe-Cr system has been a important research subject in terms of maintaining mechanical integrity of ferritic steels[1-7]. Precipitation can occur through the spinodal decomposition, and it has been reported that both mechanisms are involved in the precipitation of α'[2,3]. Effect of inhomogeneous elasticity and dislocation on Fe-Cr spinodal decomposition has been investigated[6] using the phase-field method, however the evaluation of the minimum Cr concentration at which spinodal decomposition occurs was not performed, and the quantitative microstructure analysis was also limited. In this study, we analyze effect of the dislocation on the kinetics of the spinodal decomposition, especially, the effect on the lowest nominal composition of Cr for the spinodal decomposition. Through this study, one can have more systematic understanding about α' nucleation in the presence of the dislocation. A role of the elasticity on the spinodal decomposition was analyzed by analytic approaches[8,9]. For cubic crystals, Cahn claimed that coherent elastic interaction increases the free energy, therefore, it inhibits the spinodal decomposition. On the other hand, Eshelby predicted that spinodal decomposition would be accelerated when elastic interaction was considered based on the theory of continuum elastic mechanics [9]. At first glance, it seems like a conflicting argument, Eshelby's predictions describe the rate at which spinodal decomposition occurs, and Cahn's theoretical study describes the thermodynamic conditions associated with spinodal decomposition. With the phase-field modeling, Li et al. verified that elasticity accelerates the spinodal decomposition which shows the consistency with the Eshelby's prediction [6]. In this study, we investigated whether the presence of elasticity inhibits the initiation of spinodal decomposition, as Cahn suggested [8].

All simulations are performed at the temperature T = 535K [6] using the phase-field method. Phase-field method is a method that has been actively utilized and verified to simulate the α' phase precipitation in the Fe-Cr system [6,10,11] with free energy assessed by CALPHAD approach [12]. We conducted a set of simulations by utilizing the Multiphysics Object Oriented Simulation Environment (MOOSE) framework that can easily integrate kernels such as finite element method (FEM)-based phase-field, tensor mechanics for elasticity and nucleation. The Fe-Cr microstructure modeling solver that combines the semi-implicit Fourier-Spectral method with GPU acceleration has already been developed by the authors of this paper [11], in order to consider the elastic effect and nucleation process, we determined to utilize MOOSE framework that provides a proven module. From the perspective of solving only the Cahn-Hilliard equation[13], the FEM method, which consumes intensive time to construct the mesh, takes and order longer than the spectral method. However, the constructed mesh is reused in tensor mechanics module, therefore the performance gap greatly reduces when we consider the effect of the dislocation.

2. Simulation Details

2.1 Cahn-Hilliard equation

The Cr concentration field will be evolved by solving the following Cahn-Hilliard equation [13,14]:

$$\frac{\partial \mathrm{c(r,t)}}{\partial t} = \nabla \cdot \left[M(r,t) \cdot \nabla \left(\frac{\delta F(r,t)}{\delta c} \right) \right] \tag{1}$$

$$\mathrm{F(r,t)} = \int_V \left(\left[f(c) + \frac{1}{2}\kappa(\nabla c)^2 \right] + f_e(c,r) \right) dV \tag{2}$$

The molar free energy $\mathrm{F(r,t)}$ in Eq.1 is given by Eq. 2, and $\mathrm{M(r,t)}$ is the mobility of the diffusion species. In this study, we assumed that mobility is a constant, and the value was set to 1.0.

2.2 Free energy of Fe-Cr system with dislocation

The regular-solution type chemical free energy f(c) in Eq. 2 is obtained from [15]

$$\mathrm{f(c)} = (1-c)G_{Fe}^{o} + cG_{Cr}^{o} + L_{FeCr}c(1-c) + RT(clnc + (1-c)\ln(1-c)) \tag{3}$$

where c is the composition of Cr, and G_{Fe}^{0} and G_{Cr}^{0} are the molar Gibbs free energies for the Fe and Cr, respectively. L_{FeCr} is the interaction parameter of Fe and Cr. The detailed numbers are written in [11,15]. We set the temperature T = 535K.

We determined the elastic energy density $\mathrm{f_e}(c,r)$ using Eq. 2. We implemented KHS elastic schemes [16]. The stiffness tensor and misfit strain are obtained by the interpolation and create a global stiffness tensor,

$$C_{ijkl}^{KHS}(c) = C_{ijkl,Cr} \times c + C_{ijkl,Fe} \times (1-c)$$

and the global strain is

$$\epsilon_{ij}^{KHS}(r) = \epsilon_{ij}^{tot}(r) - c \times \epsilon_{ij,\alpha'}^{o} - \epsilon_{\mathrm{ij,d}}^{o}(r) \quad (4)$$

Where $\epsilon_{ij}^{tot}(r)$ is the total strain, $\epsilon_{ij,\alpha'}^{o}$ is the eigenstrain of α' phase, and $\epsilon_{ij,d}^{o}(\mathrm{r})$ is the eigenstrain induced by the dislocation. The elastic energy is given by

$$f_e(c,r) = \frac{1}{2} C_{ijkl}^{KHS}(c)\epsilon_{ij}^{KHS}(r)\epsilon_{kl}^{KHS}(r).$$

We solve the mechanical equilibrium equation to obtain the strain-stress state as below:

$$\nabla \cdot \sigma_{ij}(r) = 0 \quad (5)$$

We utilized tensor-mechanics kernels in the MOOSE framework to solve Eq.5.

2.3. Computational details

First, we normalized the free energy in Eq. 3 by RT for computational efficiency.

$$\mathrm{f}^*(c) = \frac{f(c)}{RT}$$

We used $\kappa = 4.25$ in Eq. 2. The eigenstrain of α' phase$\epsilon_{\mathrm{ij,d}}^{o}(r)$ in Eq.4 is evaluated by [18].

$$\epsilon_{\mathrm{ij,d}}^{o}(r) = b(r) \otimes n = \frac{b_i(r)n_j + b_j(r)n_i}{2d}$$

In 2D, we assume the Burger's vector $\mathrm{b(r)} = \frac{a_0}{2}[111]$ on the connecting two dislocations on the $(1\bar{1}0)$ slip plane, where a_0 is the lattice parameter [18]. The lattice is rotated around the x-axis $[1\bar{1}0]$, y-axis [111], and z-axis $[\bar{1}\bar{1}2]$. Therefore, all terms without shear terms become 0[18]. We set $\epsilon_{12,\mathrm{d}}^{o}(r) = 0.005$ within the dislocation dipole in this study. We set $\Delta x = \Delta y = 1.0 \times 10^{-8} m$, which were implemented by $\Delta x^* = \Delta y^* = 1.0$ after normalization. The total number of meshes in the 2D system was 256×256.

3. Results

3.1. The Effect of elasticity and dislocation on α' phase precipitation induced by the spinodal decomposition mechanism.

We examined multiple compositions within the range of Fe-14Cr to investigate role of dislocation on α' precipitate nucleation through the spinodal decomposition. To examine the role of the inhomogeneous elasticity and the dislocation, we performed simulation (1) without the f_e term in Eq. 3(no elasticity case), (2) with the f_e term without dislocation (with elasticity only arising from the concentration inhomogeneity considered), and (3) with the f_e term with the dislocation..

At the initial stage, for example, in the Fe-13Cr system, 13 wt% means 13.86 at%. Therefore, we generated a fluctuated initial Cr concentration from 13.36 at% to 14.36at%. The range of the fluctuation was ± 0.05at% for all the case. First, we found that the presence of the inhomogeneous concentration did not alter the minimum Cr average concentration for the spinodal decomposition of Fe-16.7Cr; however, it altered the kinetics significantly. We observed the α' precipitate when we did not incorporate elasticity $\mathrm{t} = 14300$; on the other hand, we detected α' kinetics until $\mathrm{t} = 1732$ when we considered inhomogeneous elasticity. This observation is consistent with the predictions made by Eshelby[9].

We also found that presence of the dislocation lowered the minimum Cr concentration for spinodal decomposition. As shown in Fig.3, we found that the α' phase nucleated even in Fe-16.4Cr. As the Cr concentration increased in the vicinity of the dislocation when compared to the nominal composition, dislocation is a suitable location for the α' nucleation as experimentally observed [19]. To confirm these findings, we performed four different set of simulations with different random seeds.

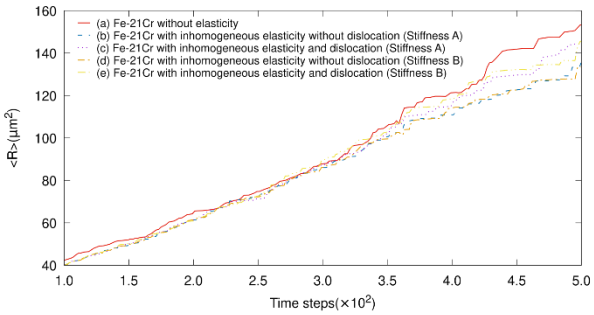

Figure 1. The average $\boldsymbol{\alpha'}$ radius ($< \mathbf{R} >$) with respect to time for the cases of (a) without elasticity, (b) with inhomogeneous elasticity without dislocation, and (c) with inhomogeneous elasticity and dislocation.

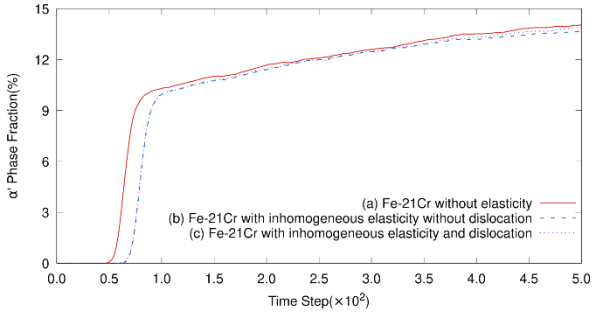

Figure 2. The $\boldsymbol{\alpha'}$ phase fraction with respect to the time for the cases of (a) without elasticity, (b) with inhomogeneous elasticity without dislocation, and (c) with inhomogeneous elasticity and dislocation.

We analyzed the role of the inhomogeneous elasticity and dislocation on the microstructural evolution of Fe-21Cr in Fig. 4. As shown in Figs. 1 and 2, when elasticity was not considered, the microstructure evolution was the fastest. When elasticity only due to the compositional

inhomogeneity was considered, the average precipitate size increased and the increased rate of the α′ phase fraction were the slowest among the three cases.

In summary, when elasticity was not considered, the system approached equilibrium the most rapidly. However, even if elasticity was considered, if the effects of structural inhomogeneity, such as dislocation, were considered simultaneously, the growth rate of the precipitate was faster in the case of the absence of the dislocation with consideration of the elasticity. At t = 70, as shown in Fig. 5(f), there was Cr concentration partitioning when a dislocation was present in the particle; therefore, a relatively large α′ precipitate existed in the vicinity of the dislocation.

In Fig. 4, we observed overshootings in the $R_m/< R >$ plot at early-stages for all three cases where R_m represents the maximum radius of the α′ phase and $< R >$ is the average radius of the α′ precipitate. In the presence of elasticity only arising from compositional inhomogeneity, transient overshooting was lower than case of the absence of the elasticity. However, with the presence of dislocation, the largest overshooting existed at approximately t = 70, where $R_m / < R >$ became smaller compared to the case of the presence of dislocation.

According to the analytic theory developed by Kawasaki and Enomoto[21], the size distribution of coarsened particles becomes wide when a repulsive elastic field is applied. As the eigenstrain is proportional to the Cr composition, we determined that repulsive elastic fields were generated between the Cr rich phases, and accordingly, the $R_m/< R >$ value was found to be larger in the presence of elasticity due to the concentration inhomogeneity without dislocation in the later stage.

In the following Fig.5, the α′ phase nucleation was more progressed in the Fe-21Cr system without elasticity (a) than in the cases with inhomogeneous elasticity at $t = 70$ ((b) and (c)). The Fe-Cr21 system with inhomogeneous elasticity and the dislocation showed more active α′ nucleation in the vicinity of the dislocation than at other sites.

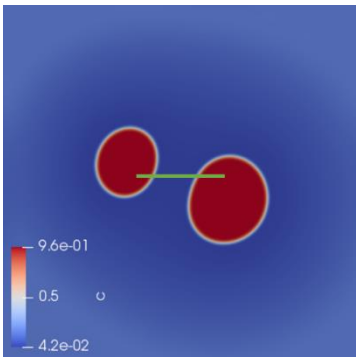

Figure 3. The $\boldsymbol{\alpha'}$ phase is nucleated in the Fe-16.4Cr system in the presence of the dislocation. The system size was $\mathbf{256 \times 256\ \mu m^2}$. The green horizontal line in the middle represents the line connecting dislocations. The microstructures were visualized by Cr composition.

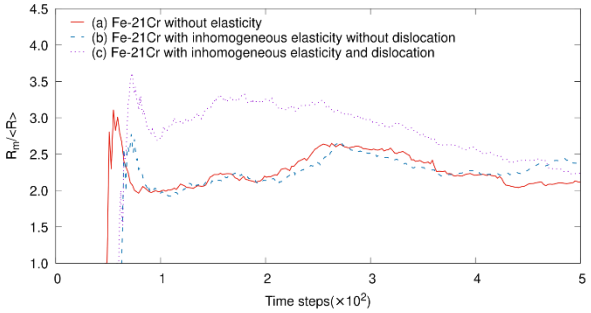

Figure 4. $\mathbf{R_m}/< \mathbf{R} >$ with respect to time for the cases of (a) without elasticity, (b) with inhomogeneous elasticity, and (c) with inhomogeneous elasticity and dislocation where $\mathbf{R_m}$ is the maximum radius of the $\boldsymbol{\alpha'}$ precipitate and $< \mathbf{R} >$ is the average radius of it. We performed four different sets of simulations to evaluate $\mathbf{R_m}$ and $< \mathbf{R} >$ for enhanced statistical rigor of the analysis. The system size was $\mathbf{256 \times 256\ \mu m^2}$. The composition of the system is 21 $\mathbf{wt\%Cr}$.

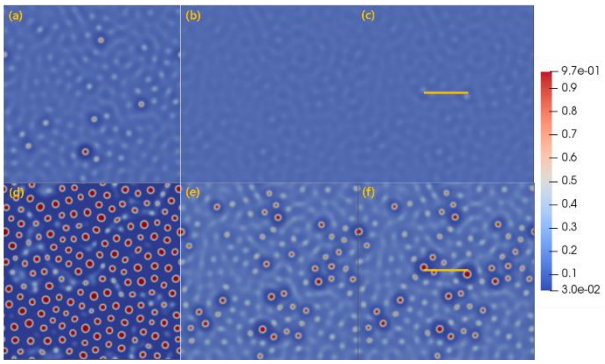

Figure 5. Microstructures of the Fe-21Cr system (a) without elasticity at t = 50, (b) with inhomogeneous elasticity without dislocation at t = 50, (c) with inhomogeneous elasticity and dislocation at t = 50, (d) without elasticity at t = 70, (e) with inhomogeneous elasticity without dislocation at t = 70, and (f) with inhomogeneous elasticity and dislocation at t = 70. The system size was $\mathbf{256 \times 256 \mu m^2}$. The microstructures were visualized by Cr composition.

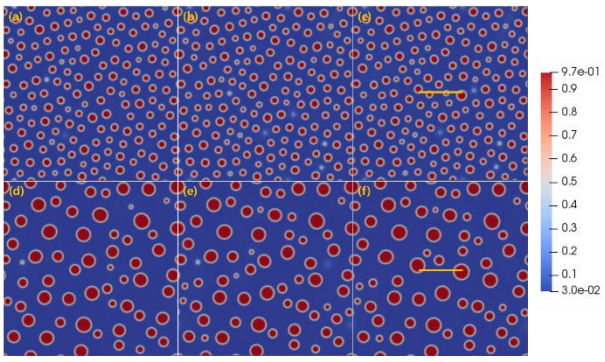

Figure 6. Microstructures of the Fe-21Cr system (a) without elasticity at t = 100, (b) with inhomogeneous elasticity without dislocation at t = 100, (c) with inhomogeneous elasticity and dislocation at t = 100, (d) without elasticity at t = 500, (e) with inhomogeneous elasticity without dislocation t = 500, and (f) with inhomogeneous elasticity and dislocation at t = 500. The system size was $\mathbf{256 \times 256 \mu m^2}$. The microstructures were visualized by Cr composition.

4. Conclusions

Phase-field simulation using the MOOSE framework has been utilized to study the effect of inhomogeneous elasticity including dislocations on α' precipitate nucleation through the spinodal decomposition in Fe-Cr alloy. Our study yields three main findings: We found that inhomogeneous elasticity induced by the compositional inhomogeneity of the α phase did not alter the minimum Cr composition for the spinodal decomposition; however, it altered the kinetics significantly. Moreover, we found that the presence of the dislocation lowered the minimum Cr composition for spinodal decomposition. At the early stage of the phase separation, the relative size of the α' precipitate was maximized when a dislocation existed in the system. In the later stage, the relative size of the precipitate showed the maximum size when inhomogeneous elasticity was incorporated without any dislocation.

REFERENCE

[1] Grobner,P. The 885 F (475 C) embrittlement of ferritic stainless steels. Metallurgical Transactions 1973, 4, 251-260.
[2] Chandra, D.; Schwartz, L. Mössbauer effect study of the 475C decomposition of Fe-Cr. Metallurgical Transactions 1971, 2, 511–519.
[3] Cieslak, J.; Dubiel, S. Nucleation and growth versus spinodal decomposition in Fe–Cr alloys: Mössbauer-effect modelling. Journal of alloys and compounds 1998, 269, 208–218.
[4] Solomon, H.; Levinson, L.M. Mossbauer effect study of 475C embrittlement of duplex and ferritic stainless steels. Acta Metallurgica 1978, 26, 429-442.
[5] Miller,M.; Hyde, J.; Hetherington, M.; Cerezo, A.; Smith, G.; Elliott, C. Spinodal decomposition in Fe-Cr alloys: Experimental study at the atomic level and comparison with computer models-I. Introduction and methodology. Acta Metallurgica et Materialia 1995, 43, 3385-3401.
[6] Li, Y.S.; Li, S.X.; Zhang, T.Y.Effect of dislocations on spinodal decomposition in Fe-Cr alloys. Journal of nuclear materials 2009, 395, 120-130.
[7] Hedstrom, P. ; Baghsheikhi, S.; Liu, P.; Odqvist, J. A phase-field and electron microscopy study of phase separation in Fe-Cr alloys. Materials Science and Engineering: A 2012, 534, 552-556.
[8] Cahn, J.W. On spinodal decomposition in cubic crystals. Acta metallurgica 1962, 10, 179-183.
[9] Eshelby, J. The continuum theory of lattice defects. In Solid state physics; Elsevier, 1956; Vol. 3, pp. 79-144.
[10] Zhu, L.; Li, Y.; Liu, C.; Chen, S.; Shi, S.; Jin, S. Effect of applied strain on phase separation of Fe-28 at.% Cr alloy: 3D phase-field simulation. Modelling and Simulation in Materials Science and Engineering 2018, 26, 035015.
[11] Lee, J.; Chang, K. Effect of magnetic ordering on the spinodal decomposition of the Fe-Cr system: A GPU-accelerated phase-field study. Computational Materials Science 2019, 169, 109088.
[12] Dinsdale, A. SGTE data for pure elements. Calphad 1991, 15, 317-425.
[13] Cahn, J.W.; Hilliard, J.E. Free energy of a nonuniform system. I. Interfacial free energy. The Journal of chemical physics 1958, 28, 258-267.
[14] Cahn, J.W. On spinodal decomposition. Acta metallurgica 1961, 9, 795-801.
[15] Andersson, J.O.; Sundman, B. Thermodynamic properties of the Cr-Fe system. Calphad 1987, 11, 83-92.
[16] Khachaturyan, A.G. Theory of structural transformations in solids; Courier Corporation, 2013.
[17] Newnham, R.E. Properties of materials: anisotropy, symmetry, structure; Oxford University Press on Demand, 2005.
[18] Biner, S.B. Programming phase-field modeling; Springer,2017.
[19] Terentyev, D.; Bergner, F.; Osetsky, Y. Cr segregation on dislocation loops enhances hardening in ferritic Fe-Cr alloys. Acta materialia 2013, 61, 1444-1453.
[20] Porter, D.A.; Easterling, K.E.; Sherif, M. Phase Transformations in Metals and Alloys, (Revised Reprint); CRC press, 2009.
[21] Kawasaki, K; Enomoto, Y. Statistical theory of Ostwald ripening with elastic field interaction. Physica A: Statistical Mechanics and its Applications 1988, 150, 463-498.